Available online at www.sciencedirect.com
SCIENCE DIRECT®
Catalysis Today 85 (2003) 291–301
CATALYSIS TODAY
www.elsevier.com/locate/cattod

H_2S adsorption on polycrystalline UO_2

Qifei Wu [a], Boris V. Yakshinskiy [a], Thomas Gouder [b], Theodore E. Madey [a,*]

[a] *Laboratory for Surface Modification, Department of Physics and Astronomy, Rutgers, The State University of New Jersey, Piscataway, NJ 08854, USA*
[b] *European Commission, Joint Research Centre, Institute for Transuranium Elements, Postfach 2340, D-76125 Karlsruhe, Germany*

Abstract

We report results on the adsorption and desorption of H_2S on polycrystalline UO_2 at 100 and 300 K, using ultrahigh vacuum X-ray photoelectron spectroscopy (XPS), low energy ion scattering (LEIS), and temperature programmed desorption (TPD). Our work is motivated by the potential for using the large stockpiles of depleted uranium in industrial applications, e.g., in catalytic processes, such as hydrodesulfurization (HDS) of petroleum. H_2S is found to adsorb molecularly at 100 K on the polycrystalline surface, and desorption of molecular H_2S occurs at a peak temperature of ∼140 K in TPD. Adsorption rates of sulfur as a function of H_2S exposure are measured using XPS at 100 K; the S 2p intensity and lineshapes demonstrate that the saturation coverage of S-containing species is ∼1 monolayer (ML) at 100 K, and is ∼0.3–0.4 ML of dissociation fragments at 300 K. LEIS measurements of adsorption rates agree with XPS measurements. Atomic S is found to be stable to >500 K on the oxide surface, and desorbs at ∼580 K. Evidence for a recombination reaction of dissociative S species is also observed. We suggest that O-vacancies, defects, and surface termination atoms in the oxide surface are of importance in the adsorption and decomposition of S-containing molecules.

Keywords: Adsorption; Hydrogen sulfide; Uranium oxide; X-ray photoelectron spectroscopy; Temperature programmed desorption

1. Introduction

In the petroleum industry, metal oxides are widely used as catalyst substrates for desulfurization and denitrogenation [1,2]. A typical commercial hydrodesulfurization (HDS) catalyst consists of Al_2O_3 (support) and Ni- or Co-promoted MoS_2 or WS_2 (catalyst); such catalysts have been used for over 50 years [1,3]. The Al_2O_3 substrate is believed to be thermally stable under industrial HDS conditions (∼600 K, 100 atm) and capable of greatly increasing the surface area of the catalyst. However, because of the low yield in desulfurizing aromatic S-containing molecules, e.g. thiophene, there is increasing interest in understanding the fundamental mechanisms of HDS, and in searching for the next generation of HDS catalysts (so-called deep hydrodesulfurization). Efforts include developing new materials with catalytically active sites and new oxide support systems [1,4–12]. In particular, Ramirez et al. found that in a TiO_2 supported HDS catalyst system, titanium species can promote the catalytic Mo/W phase, giving rise to a synergistic effect [6,7]. Wang et al. and Kogan et al. employed ^{35}S to trace the behavior of S on TiO_2 supported and $CoMo/Al_2O_3$ sulfide HDS catalysts [8–10]. In the industrial HDS process [1], S-containing molecules react with hydrogen over the surface of a catalyst, and S is removed or desorbed as H_2S. Hence, the interactions of H_2S with HDS catalysts, e.g. adsorption and desorption characteristics, are crucially important in

* Corresponding author. Tel.: +1-732-4455185; fax: +1-732-4454991.
E-mail address: madey@physics.rutgers.edu (T.E. Madey).

0920-5861/$ – see front matter © 2003 Elsevier B.V. All rights reserved.
doi:10.1016/S0920-5861(03)00395-X

mechanistic studies. For instance, Leglise et al. used H_2S as a tool for evaluating the HDS activities of commercial $CoMo/Al_2O_3$ catalysts [13].

There are increasing numbers of fundamental studies on the understanding of metal oxide surface chemistry (e.g., role in HDS) in the last 20 years [14]. Properties of metal oxides are of considerable interest in many industrial applications, including microelectronics, superconductivity, and heterogeneous catalysis; the technical importance of metal oxides and relevant interfaces have been reviewed and discussed experimentally and theoretically [15,16]. However, many issues about the surfaces of certain metal oxides are not well understood yet, e.g. identity of termination atoms, defect structure, and surface reconstructions. For example, since elemental metal oxides are binary systems, the termination atoms of an oxide surface can vary from one crystallographic orientation to the other [14], and even as a function of gas composition, pressure and temperature [17]; this can lead to very different chemical properties in adsorption studies. In terms of the importance of defects on oxide surface, Kim, Goodman et al. recently reported differences in the reactivity of a well-ordered MgO(1 0 0) in comparison with a defective MgO(1 0 0) [18,19]. Careful surface preparation and treatment of metal oxides is thus important to obtain reliable data. Concerning the role of metal oxides in industrial desulfurization reactions, surface studies have emerged recently for the interactions of H_2S, SO_2, S_2, and thiophene with metal oxides, such as TiO_2, ZnO, MgO, and Cr_2O_3 [4,20–28]. The experimental methods employed include synchrotron radiation based soft X-ray photoelectron spectroscopy (SXPS), ultraviolet photoelectron spectroscopy (UPS), temperature programmed desorption (TPD), electron stimulated desorption (ESD), low energy electron diffraction (LEED), and scanning tunneling microscopy (STM). It is believed that O sites and vacancies on the surface can play an important role in the initial replacement reaction between adsorbed S molecules/fragments and surface O [22,27,28].

Large stockpiles of depleted uranium are stored in the US; the potential use of depleted uranium in industry, e.g. for catalytic reactions, is motivated by a desire to convert a negative value material to positive one. In the last decade, uranium oxides (e.g. UO_2) were discovered to demonstrate catalytic properties in the oxidative destruction of toxic volatile organic compounds (VOCs), such as butane, benzene, chlorobenzene, and other chlorine containing molecules [29,30]. UO_2 has been used as a catalytic support for steam reforming of methane [31]. Remarkably, Madhavaram and Idriss found direct formation of furan from acetylene over polycrystalline β-UO_3 [32]; the reactions of carboxylic acids on UO_2(1 1 1) single crystal surfaces were also investigated [33]. However, studies of uranium oxides are complicated: the bulk structures of uranium oxides show a transition from face centered cubic (fcc) fluorite to layered structures when the oxidation states of uranium in the oxides change [34]. UO_2 has remarkable accommodation ability for O atoms, based on the availability of interstitial sites and vacancies. It has been suggested that the relaxation of oxygen atoms on UO_2(0 0 1) is not limited to the topmost layer but includes the outermost two or three atomic layers [35]. The preparation of clean surfaces of UO_2 is important to assure a stable and reproducible substrate and to obtain reliable data. Recently, we have performed an adsorption study of H_2S on single crystal of UO_2 with (0 0 1) orientation [36]. We found that hydrogen sulfide (H_2S) is weakly bonded to the uranium oxide surface and the saturation coverage of S-containing species is ∼1 monolayer (ML) at 100 K, and decreases with increasing temperature to ∼0.2 ML of dissociation fragments at 300 K. In this work, we extend our study to an interesting form of uranium oxides more relevant to catalysis, polycrystalline UO_2, and measure the adsorption chemistry of H_2S on the surface. We find that both U sites and O sites on the polycrystalline surface participate in the adsorption of H_2S, and different desorption channels of S species are explored. Implications of UO_2 for possible HDS catalysis are summarized.

2. Experiments

The detailed experimental setup has been described previously [36,37]. All experiments are done in an ultrahigh vacuum (UHV) chamber containing instrumentation for XPS, LEIS, TPD, and ESD, with base pressure $<6 \times 10^{-9}$ Pa. A polycrystalline UO_2 sample is prepared in Karlsruhe by sputtering UO_2 onto a Mo substrate and forming a thin film $\sim 10^3$ Å in thickness. The sample is mounted to tantalum (Ta) wires by

spot-welding; a cromel/alumel thermocouple is also spot-welded to the sample edge for temperature measurement. The sample can be resistively heated, and cooled to ~100 K using liquid nitrogen (LN_2). Typically, the polycrystalline UO_2 sample is cleaned first by 1 keV Ar^+ sputtering for 5 min, then annealing at ~600 K in an atmosphere of oxygen (1×10^{-5} Pa) for 5 min, and held at the same temperature for an additional 3 min after pumping away the oxygen. The cleanliness and stoichiometry of the sample are monitored using LEIS (1 keV He^+) and XPS (Al Kα). Usually, we use a grazing angle (~60° from surface normal) of the CHA analyzer in collecting XPS data to enhance surface sensitivity; the scattering angle of He^+ beam in LEIS measurements is 135°. H_2S gas is dosed onto the sample via a gas doser capped by a capillary array, which provides a flux enhancement of ~20× higher than the background flux at the same chamber pressure according to XPS measurements. Note that in the following Section 3, H_2S doses in Langmuir are expressed as effective doses (~20 times the background flux; $1\,L = 1.3 \times 10^{-4}$ Pa s). The purity of H_2S gas is monitored with a quadrupole mass spectrometer (QMS) that is also used for TPD measurements (heating rates of 3–4 K/s) and for detection of ions in ESD.

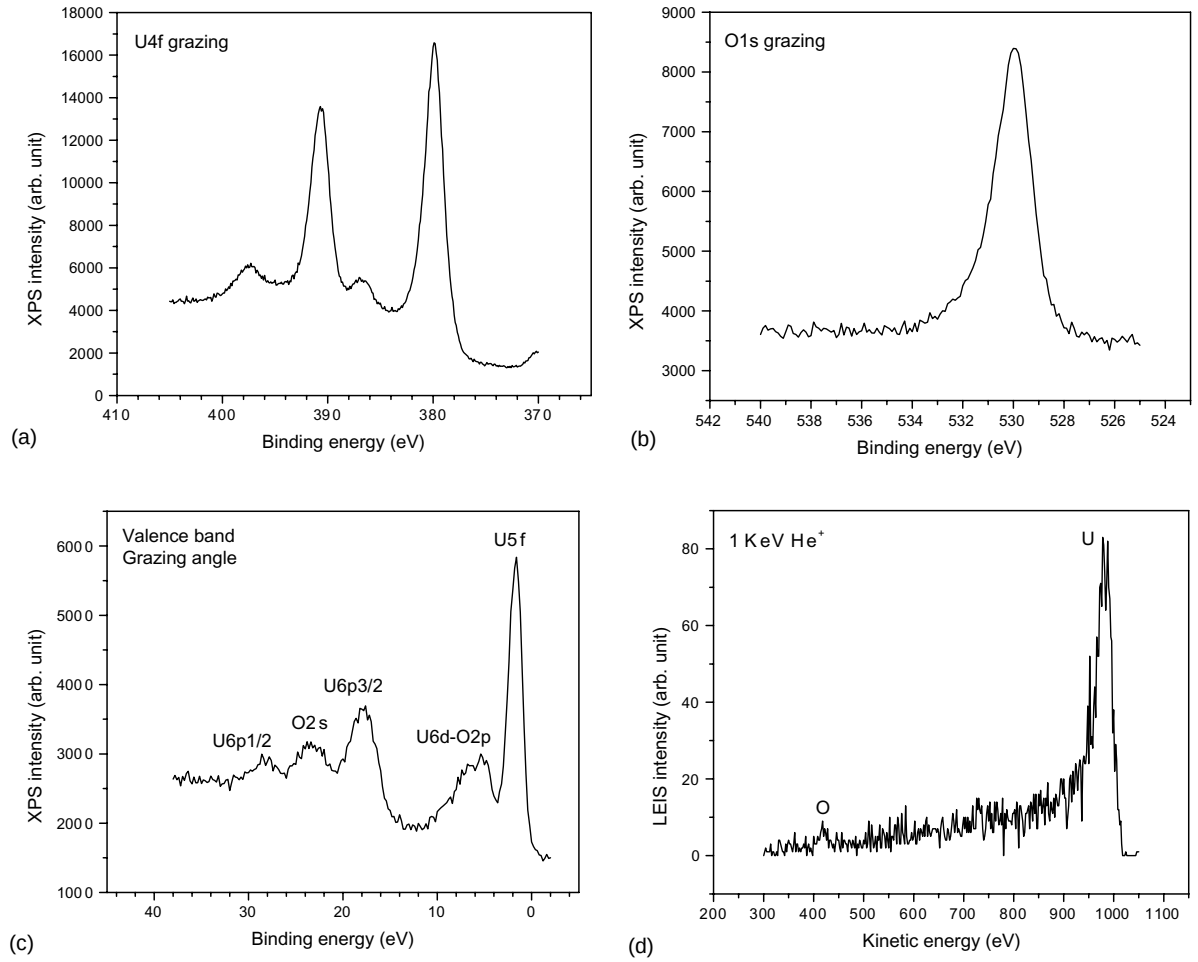

Fig. 1. Characterization of the clean polycrystalline UO_2 surface: (a) grazing angle XPS of U4f; (b) grazing angle XPS of O1s; (c) grazing angle XPS of the valence band; (d) LEIS spectrum of U and O. For all XPS spectra (a) to (c), the analyzer is operated in the FAT 22 mode.

3. Results

3.1. Characterization of clean polycrystalline UO_2

We have characterized the clean surface of polycrystalline UO_2 (poly-UO_2) using XPS and LEIS, and the results are plotted in Fig. 1. Both grazing angle U $4f_{5/2}$ (391 eV) and U $4f_{7/2}$ (380 eV) are accompanied by satellite shake-up features, located about 7 eV higher in binding energy than the main peaks; this satellite structure is a fingerprint of stoichiometric UO_2 [37,38]. The asymmetrical feature at the high binding energy side of O 1s peak (Fig. 1b) is also seen on the UO_2(0 0 1) surface [37]. Valence band structure (Fig. 1c) is consistent with our previous publication for UO_2(0 0 1) [37]; however, the relative intensities of specific peaks are different, apparently due to different surface structures and termination atoms. In particular, the O 2s intensity is lower than that found on UO_2(0 0 1), implying that surface oxygen is less abundant on the poly-UO_2 sample or the chemical environment of surface oxygen is different. An LEIS spectrum (Fig. 1d) exhibits a large U peak and a small O peak, in agreement with data for UO_2(0 0 1) [36]; since uranium is a high-Z atom, its He^+ LEIS intensity is expected to be much higher than that of O.

3.2. Adsorption of H_2S on polycrystalline UO_2

Fig. 2a shows a series of grazing angle XPS spectra for the S 2p region, as the effective dose of H_2S on poly-UO_2 increases from 0.04 to 8.4 L at 100 K. The sulfur feature that appears at the lowest exposures is a broad peak centered at ~162.5 eV (see 0.04 L spectrum). Starting at 0.2 L dose, a new peak at ~164.5 eV becomes noticeable and increases in intensity with increasing H_2S dose. When H_2S is dosed onto poly-UO_2 at 300 K, we find that a much larger dose of H_2S is needed to obtain a noticeable S2p XPS peak. Fig. 2b shows the S 2p spectra after dosing 400 and 800 L H_2S at room temperature (note that the intensity scales are different in Fig. 2a and b). The S 2p peaks also appear at ~162.5 eV, consistent with the S 2p feature at the lowest doses of H_2S at 100 K. It is generally believed that H_2S adsorbs dissociatively on metal oxides at room temperature [23,24,36,39], and the measured binding energy of S $2p_{3/2}$ for adsorbed dissociative S species is reported

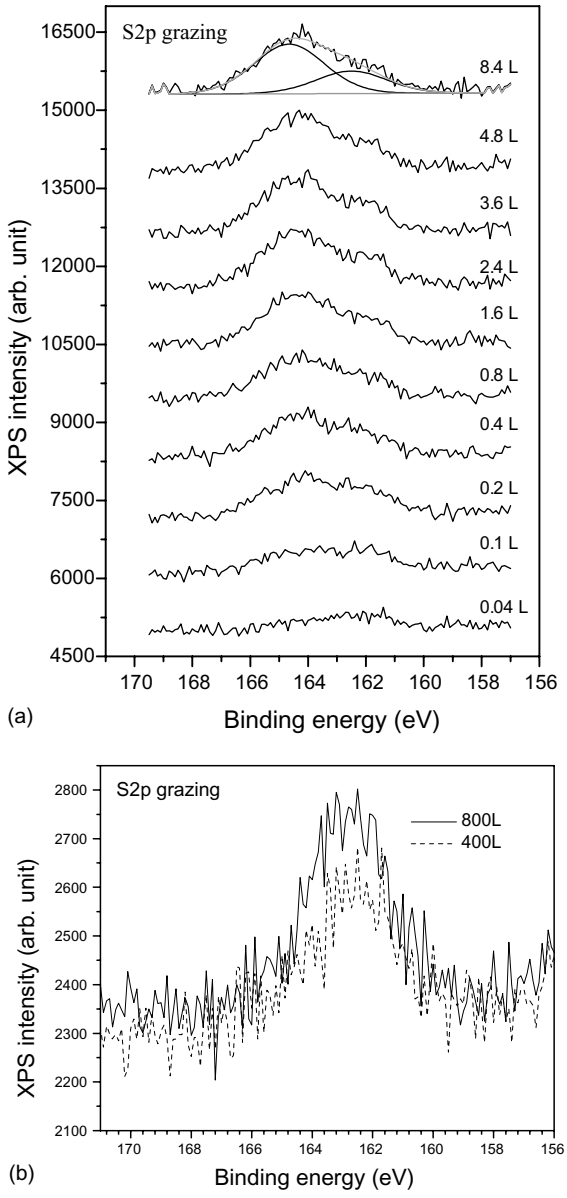

Fig. 2. (a) Grazing angle XPS of S2p as a function of H_2S dose at 100 K. At the lowest dose (0.04 L), a broad peak centered at 162.5 eV is the dominant feature of S2p, whereas a higher binding energy peak (~164.5 eV) develops with increasing dose up to 8.4 L. (b) Room temperature adsorption of 400, 800 L H_2S on clean poly-UO_2 surface. Note the different intensity scales for (a), (b). For all XPS spectra in (a) to (b), the analyzer is operated in the FAT 44 mode.

to be ∼162 eV using high resolution SXPS [23,24]. The topmost curve in Fig. 2a (8.4 L) is fit well using two Gaussian peaks, each with full width at half maximum (FWHM) of 3 eV. One peak at 162.5 eV also fits the data of Fig. 2b; the second peak is at 164.5 eV. Note that all curves of Fig. 2a can be fit using the same two peaks. The S $2p_{3/2}$ and $2p_{1/2}$ features are not resolved. Based on the above observations, we suggest that the peak centered at ∼162.5 eV in Fig. 2a and b corresponds to dissociation fragments of H_2S (i.e. S, SH); the peak at ∼164.5 eV in Fig. 2a is associated with molecular H_2S. As discussed below, this assignment is consistent with the TPD measurements.

Fig. 3 shows grazing angle XPS spectra of U 4f and O 1s before and after H_2S dose at 100 K. Neither peak exhibits significant chemical shift, however, the peak intensities are attenuated slightly as the surface is covered by adsorbate.

The integrated uptake of S-containing species on poly-UO_2 as a function of H_2S dose can provide direct information about the adsorption kinetics of H_2S. Fig. 4 demonstrates the normalized XPS intensity of S 2p, U 4f, and O 1s as a function of effective H_2S dose at 100 K (the normalized XPS S 2p vs. dose at 200 K is drawn as a dashed line). The S 2p intensity increases quickly at low exposures, but slows down above ∼1 L dose as the saturation level of H_2S is approached at 100 K. The saturation level of S 2p at 200 K is less than half of that at 100 K. For U 4f and O 1s, both normalized intensities decrease noticeably at doses <1 L.

Fig. 5a shows plots of the LEIS spectra for U, O, and S with increasing H_2S dose from 0.1 to 5 L at 100K; Fig. 5b shows the normalized intensity of U, O, and S as a function of effective H_2S dose (the intensity of U is normalized according to the peak height on the high kinetic energy side; the intensities of O and S are normalized according to the corresponding peak areas). The adsorption rate of S and the attenuation of U and O (Fig. 5) are consistent with the observations by XPS (Fig. 4). Note, however, that LEIS is much more sensitive to the topmost layer of UO_2 than is XPS; consequently, attenuation of surface features by H_2S is more noticeable in LEIS data (Fig. 5). Both LEIS and XPS results suggest that S species are adsorbed on both U and O sites; this is very different from the study on single crystal UO_2(0 0 1) where S species are found to adsorb preferentially on O sites [36]. Based on the rate of uptake of S in Figs. 4 and 5 we estimate that the

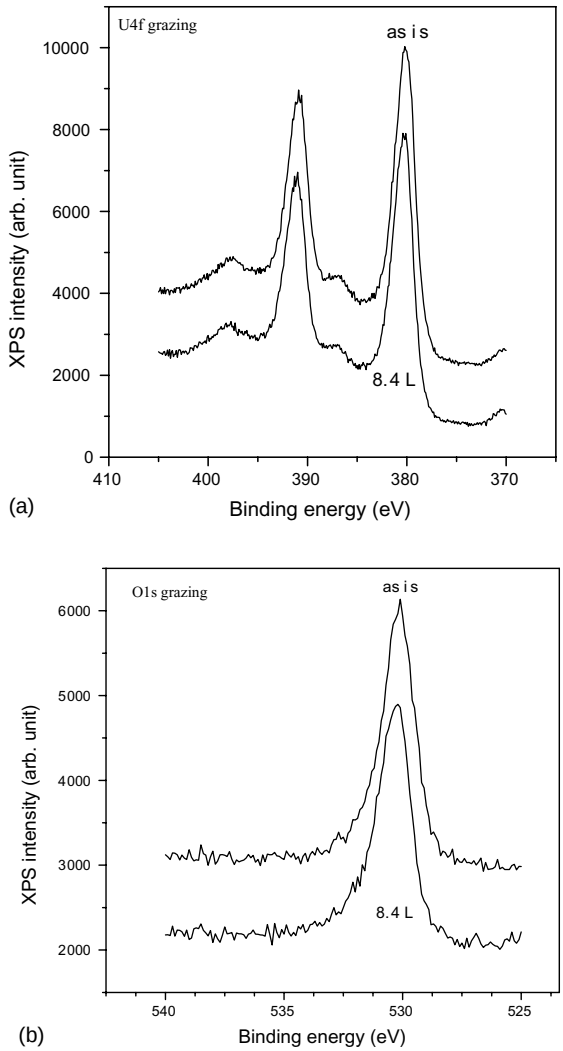

Fig. 3. Grazing angle XPS of U4f and O1s before and after dosing 8.4 L H_2S at 100 K.

initial sticking probability is ∼1. The saturation coverage of S species on polycrystalline UO_2 is ∼1 ML at 100 K (Figs. 2–5); the maximum coverage of dissociative S species is about 0.3–0.4 ML at room temperature, for effective doses of 400–800 L (Fig. 2b).

3.3. Thermal desorption of H_2S and atomic S from polycrystalline UO_2

We have studied the thermal desorption of H_2S systematically. Fig. 6a shows a series of TPD spectra

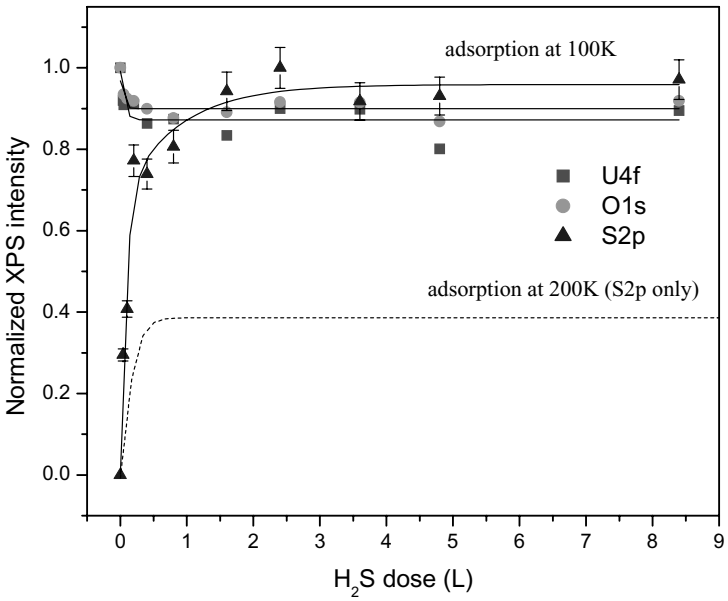

Fig. 4. Uptake of S2p (100 and 200 K) and attenuation of U4f and O1s (100 K) as a function of H_2S dose.

for molecular H_2S (mass 34) following adsorption of H_2S onto the substrate held at 100 K. Each spectrum of Fig. 6a is obtained for an initially clean poly-UO_2 surface. At the lowest H_2S dose (0.04 L), the thermal desorption peak has low intensity and the peak temperature is ∼250 K. Starting from 0.1 L dose, another desorption peak at lower temperature (∼150 K) appears, and increases its intensity with increasing H_2S dose. The lower-temperature desorption peak is ascribed to molecularly adsorbed H_2S on poly-UO_2, as observed before on UO_2(0 0 1) [36]. By dosing the poly-UO_2 sample with a saturation coverage of H_2S (10 L) and then annealing to specific temperatures indicated by A–E, the thermal desorption kinetics are also monitored by XPS S 2p, as shown in the inset of Fig. 6a. TPD and XPS results agree with each other: first, desorption of molecularly adsorbed H_2S at 140 K corresponds to the disappearance of S 2p at 164.5 eV in XPS spectra; second, the XPS S 2p peak at ∼162.5 eV decreases with increasing temperature, consistent with the continuing desorption of H_2S associated with recombination of dissociatively adsorbed H_2S fragments on the surface (as discussed in Section 4). Following adsorption of H_2S at room temperature, we also observe the thermal desorption of molecular H_2S (mass 34) from the surface, as shown in Fig. 6b. Since there is no XPS evidence for molecularly adsorbed H_2S on the surface at 300 K (cf. Fig. 2b), the thermal desorption of H_2S in Fig. 6b is associated with a surface recombination reaction. A similar situation is also identified in TPD spectra of H_2S at the lowest exposures at 100 K (in Section 3.2, we show evidence that H_2S exists as dissociation fragments at ∼0.04 L dose): the thermal desorption at ∼250 K may also be due to a recombination reaction of dissociative H_2S fragments. Based on the Redhead equation [40,41] for first order desorption, and assuming a preexponential of $10^{13}\,s^{-1}$, we estimate that the desorption energy of molecular H_2S corresponding to the peak at 140 K is ∼35 kJ/mol. If we compare the TPD peak area for molecular H_2S in Fig. 6a with the XPS S 2p peak area in Fig. 2, the relation between the concentration of molecularly desorbed H_2S and the concentration of S-containing species on the surface can be plotted; this is shown in Fig. 6c. The non-linear character of this plot supports the conclusion that at the lower H_2S doses, a fraction of the adsorbed species are dissociated and do not desorb as molecular H_2S.

To provide further insights into the dissociation products of H_2S on poly-UO_2, we have searched for

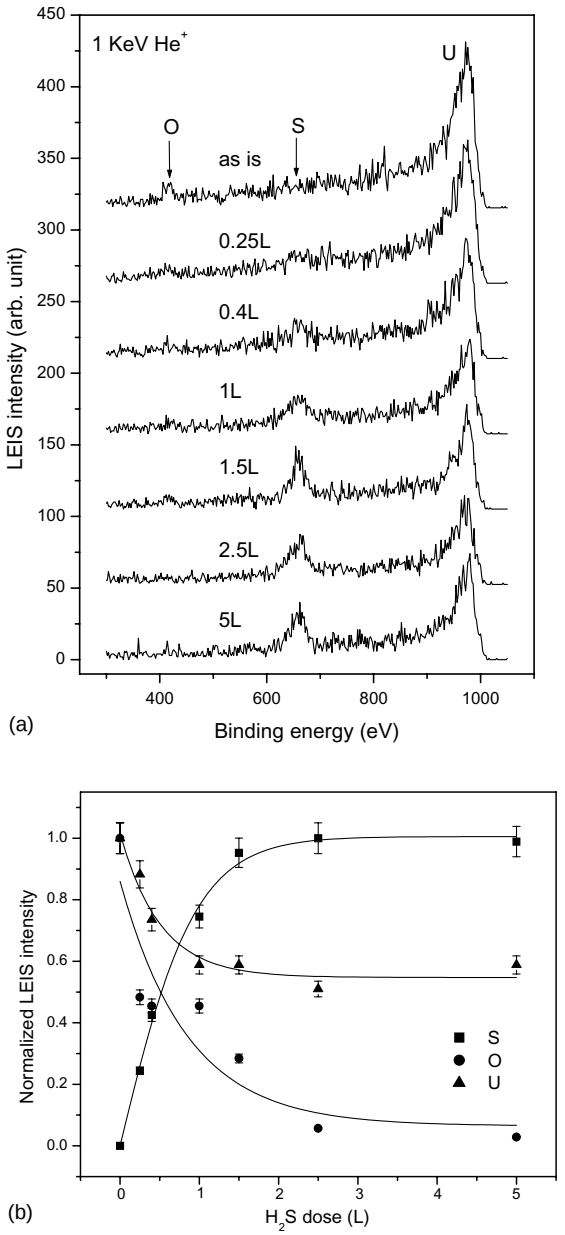

Fig. 5. (a) LEIS spectra of H_2S covered UO_2 surface with increasing H_2S dose at 100 K. (b) Variation of normalized LEIS S, O, U intensity as a function of H_2S dose.

the thermal desorption of atomic S and molecular SO_2; the TPD signal from mass 64 (SO_2) is negligible. Fig. 7a shows a thermal desorption spectrum for atomic S (mass 32) from poly-UO_2 dosed with ∼3 L H_2S and preheated to <500 K (in this way, molecular H_2S is first thermally removed, and the thermal desorption of atomic sulfur exhibits a pronounced peak). The atomic sulfur peak is noisy, because atomic sulfur is a small fraction of S species on the surface (∼0.1 ML, based on XPS S 2p intensity). Another approach is to repetitively heat (<500 K) and dose H_2S onto the poly-UO_2 surface, and we found that this is an efficient way to built-up dissociative S species on the surface. Fig. 7b demonstrates the thermal desorption of atomic S (mass 32) after 5 heating–dosing cycles, followed by a final dosing of the surface with 5 L H_2S at 100 K. Note that a thermal desorption peak at ∼140 K is observed because of the cracking of H_2S molecules in the QMS ion source during heating. Accordingly, Fig. 7b is a full TPD spectrum containing two peaks: one (140 K) originating from thermal desorption of molecular H_2S and the other (580 K) from thermal desorption of accumulated atomic S. Based on measurements of S 2p intensity for atomic S after comparable repetitive heating-dosing cycles, we estimate that ∼0.4–0.5 ML of atomic S desorbs from the surface. Also, the thermal desorption peak at 580 K in Fig. 7b (after heating–dosing accumulation) is ∼5 times more intense than that in Fig. 7a. The binding energy of atomic S (assuming first order desorption, and using the Redhead equation [40]) is ∼150 kJ/mol.

The chemical species on the H_2S-dosed poly-UO_2 surface after different temperature treatments can also be characterized by LEIS. Fig. 8a shows LEIS spectra after heating below (470 K) and above (680 K) the desorption temperatures of atomic S. Initially the substrate uranium peak and oxygen peak are both attenuated by a saturation dose of H_2S at 100 K (>5 L, Fig. 8a(ii)). Before the final saturation dosing, several heating-dosing cycles are performed, similar to the conditions used in Fig. 7b. After a gentle heating (∼470 K, Fig. 8a(iii)), we find that the U peak is first restored, comparable to the intensity of the U peak before dosing H_2S. However, there is still considerable atomic sulfur on the surface, as shown below in Fig. 8b. After further heating (∼680 K, Fig. 8a(iv)), the LEIS O signal is also restored, due to the thermal desorption of atomic S (Fig. 7); however, diffusion of S deep into the bulk of poly-UO_2 may also be possible. Fig. 8b shows grazing angle XPS spectrum of S 2p after the accumulation of atomic sulfur and a further heating to remove molecular H_2S.

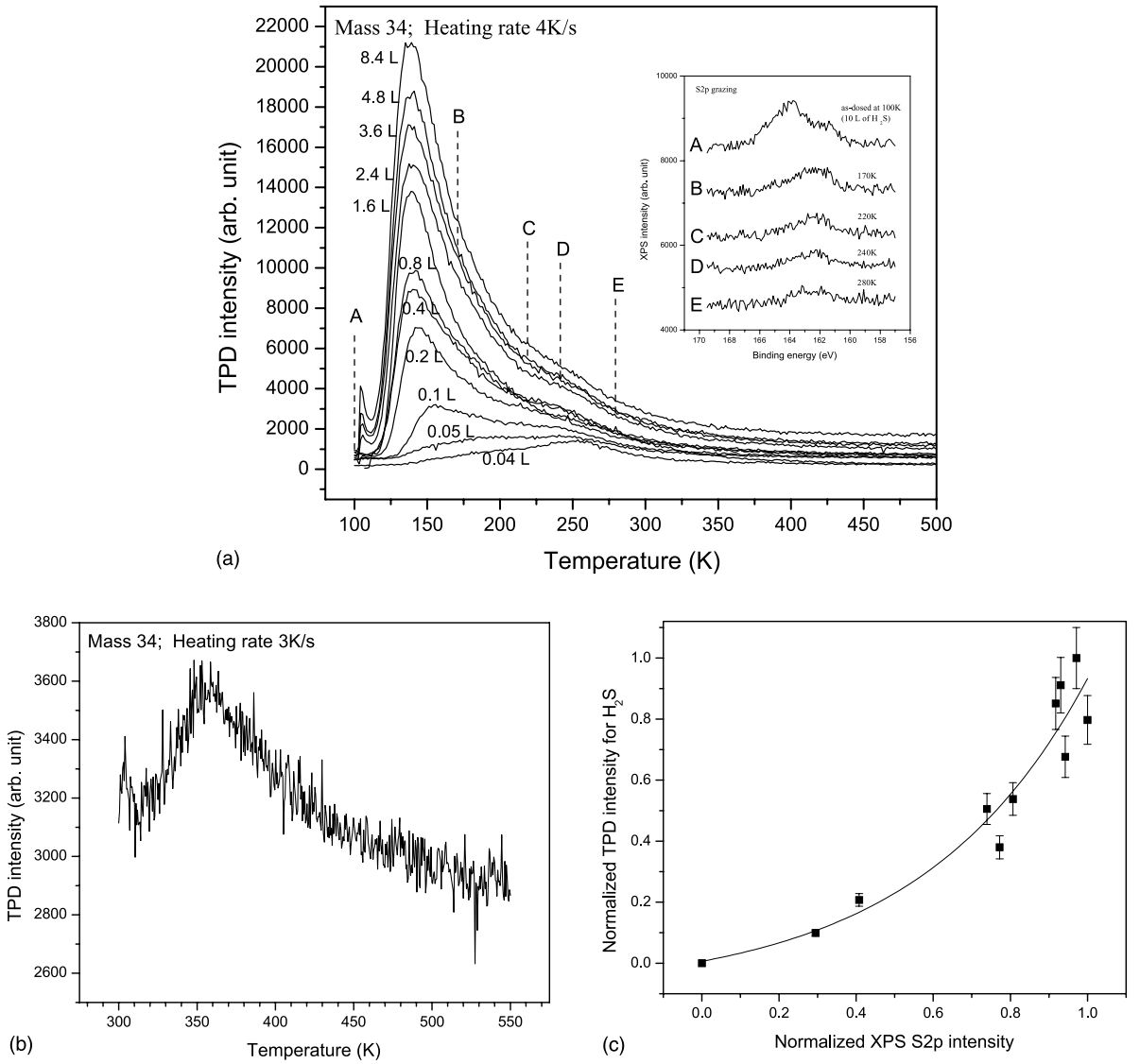

Fig. 6. (a) Temperature programmed desorption (TPD) of molecular H_2S (mass 34) corresponding to increasing H_2S dose onto clean UO_2 at 100 K. The inset shows the corresponding XPS spectra when the H_2S saturated (10 L) sample is heated to various temperatures for ~15 s, then cooled to 100 K for XPS measurements (A, as-dosed; B, 170 K; C, 220 K; D, 240 K; E, 280 K). (b) TPD for molecular H_2S (mass 34) following adsorption of H_2S at 300 K. The desorption of H_2S is associated with a recombination reaction of dissociated H_2S fragments. (c) Correlation of XPS S2p area and TPD area for molecular H_2S at different H_2S doses.

The center of the peak is ~162.5 eV, indicating the presence of built-up dissociative S species. We estimate the amount of atomic sulfur to be ~0.5 ML by comparing to Fig. 2a; the result is consistent with the LEIS spectrum in Fig. 8a(iii) and TPD spectrum in Fig. 7b.

4. Discussion

Based on our TPD and LEIS measurements in different temperature ranges, we have an understanding of chemical states of sulfur on poly-UO_2 and the thermal desorption channels from the surface. From the

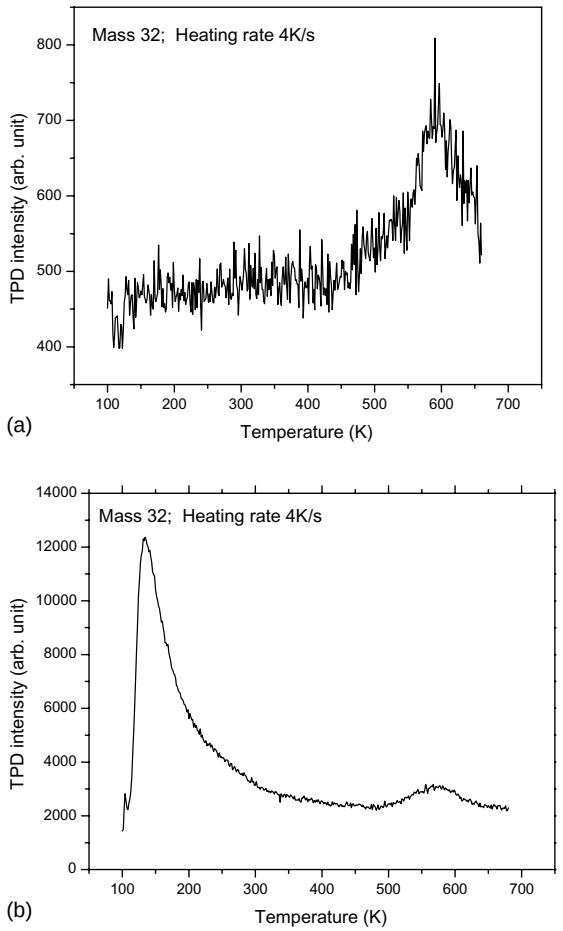

Fig. 7. TPD for atomic S (mass 32): (a) surface prepared by dosing 3 L H_2S followed by heating to 500 K to desorb molecular species; (b) surface prepared by multiple doses of H_2S (sum of doses >10 L) followed by heating (<500 K), and a final dosing of 5 L H_2S.

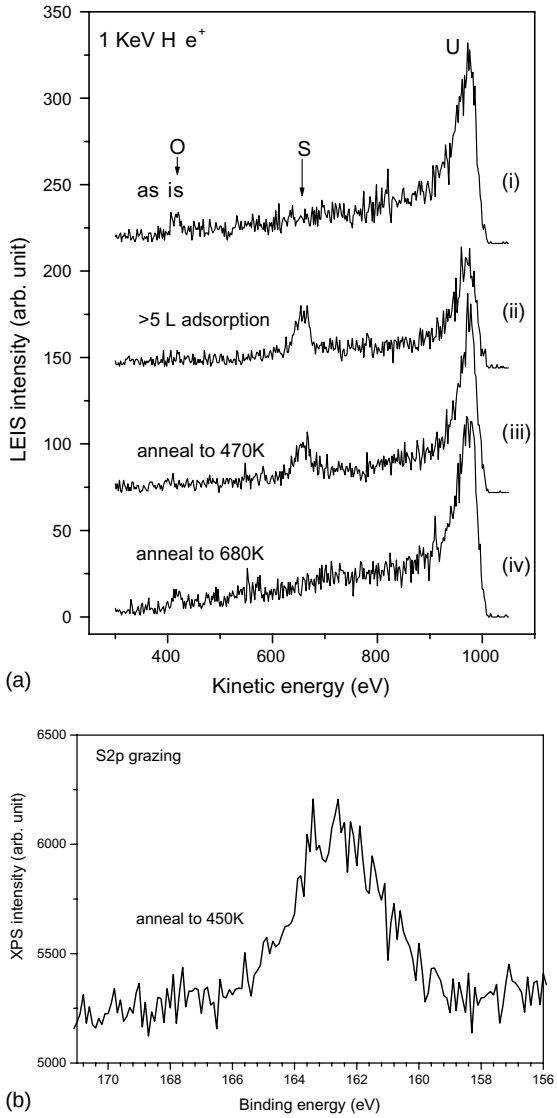

Fig. 8. (a) LEIS spectra of UO_2 surface when the surface is (i) clean, (ii) dosed with >5 L dose (saturation) of H_2S after heating-dosing cycles at 100 K, (iii) heated to 470 K, and (iv) heated to 680 K. (b) Grazing angle XPS of S2p after the atomic sulfur is accumulated through heating-dosing cycles and a final heating to 450 K, under similar conditions to (a(iii)).

XPS and LEIS uptake studies, we find that S species are adsorbed on both U sites and O sites on poly-UO_2, and attenuate both signals. Based on the LEIS measurements in Fig. 8, it is suggested that S species on U sites are mostly associated with weakly bonded H_2S molecules and S species on O sites are mainly associated with strongly bonded dissociative S species. Weakly adsorbed H_2S molecules on U sites may experience a bonding contribution from electrostatic interactions between U cationic sites and H_2S dipoles. Strongly bonded S species may exist on the surface or subsurface through replacement of O atoms at these positions and by diffusion of O-vacancies from the bulk during annealing. In the initial stages of H_2S adsorption, surface defect sites and O-vacancies are believed to be the first sites to dissociate and stabilize S species [22,28]; however, dissociation at cation sites to form USH species cannot be eliminated. When the

poly-UO_2 surface saturated by H_2S at 100 K is heated, our evidence suggests that the thermal desorption of S species occurs via the following scenario. Direct desorption of weakly bonded molecular H_2S is the first channel to occur, at ∼140 K (Fig. 6a). Upon heating to slightly higher temperature, e.g. 250 K, a recombination reaction takes place, i.e. [42]:

$$2SH \rightarrow H_2S + S$$

This disproportionation reaction contributes to further desorption of H_2S (mass 34, Fig. 6a) and also leads to accumulation of atomic S. Finally, atomic S (mass 32) can be thermally desorbed at ∼580 K, but a further diffusion of atomic S into the bulk is also possible. The recombination channel of SH species provides a plausible mechanism for the accumulation of atomic S during heating–dosing cycles: heating (<500 K) gives rise to the production of atomic sulfur, and also accelerates the diffusion of O-vacancies to the surface. Thus, more active sites for further adsorption and decomposition of H_2S are created.

We have previously studied the adsorption and decomposition of H_2S on single crystal UO_2(0 0 1) [36]. When comparing the results above with those for UO_2(0 0 1), we find both similarities and differences. On polycrystalline UO_2, both O sites and U sites demonstrate reactivity towards H_2S, but O sites are the preferred sites for the adsorption of H_2S on single crystal UO_2(0 0 1). From XPS measurements at the saturation coverage (∼1 ML) at 100 K, an XPS S2p with a width of ∼8 eV (Fig. 2a) is observed for polycrystalline UO_2 and a broader XPS S2p (∼10 eV) is found for the UO_2(0 0 1) single crystal. Differences are also identified in room temperature adsorption studies: the adsorption of dissociated S species can reach about 0.3–0.4 ML on poly-UO_2, whereas only 0.2 ML on single crystal UO_2(0 0 1) is estimated. Defect and O-vacancy structures on these two surfaces are different, manifesting different chemical reactivity. The poly-UO_2 surface can be mimicked to be several micro-surfaces/facets of UO_2 with different orientations, whereas single crystal UO_2(0 0 1) contains just one orientation with more uniform termination. It appears that abundant uranium cations on poly-UO_2 may be exposed to H_2S gas molecules during dosing, but oxygen anions are the predominant contact atoms with H_2S on single crystal UO_2(0 0 1). Excess oxygen on UO_2(0 0 1) could even possibly oxidize some adsorbed H_2S molecules and lead to the formation of SO_x species, as described before [36]. A surface model of UO_2(0 0 1) was proposed previously based on LEED, LEIS, and XPS measurements [37,43,44], suggesting that the surface is terminated by 1 ML oxygen in a zigzag pattern along ⟨1 1 0⟩ direction. Structures of UO_2 surfaces with other orientations were investigated using LEED, LEIS, and STM: on UO_2(1 1 0), uranium and oxygen appear to be coplanar and U sites are visible in STM images [43,45]; the outermost layer of UO_2(1 1 1) is dominated by oxygen, although the observed atoms in STM images are assigned as uranium because of density of states (DOS) considerations [46,47].

Whether or not UO_2 surfaces can be used industrially for HDS catalysts (presumably as catalyst supports) is still an open question. Our studies indicate that UO_2 surfaces demonstrate a mild reactivity towards H_2S. The accumulation of atomic sulfur on UO_2 surface/subsurface through atom diffusion/replacement and regeneration of clean UO_2 surface during heating to ca. 600 K are interesting processes, considering that S vacancies are believed to play the key roles in catalytically active phases under industrial HDS conditions (∼600 K, 100 atm) [1]. However, in order to develop a good support for HDS catalysts, other effects such as mechanical stability, economic factors, and safety (even depleted uranium has residual radioactivity) need also to be taken into account. It may be possible that a support system consisting of an oxide mixture (e.g. UO_2 and Al_2O_3) could enhance the performance of HDS catalysts in the desulfurization of aromatic S-containing molecules. Catalytic scientists have found that supports based on TiO_2–Al_2O_3 mixed oxides demonstrate satisfactory HDS activity towards thiophene and a synergistic effect is proposed based on the presence of reduced titanium species, which possibly change the dispersion and morphology of the catalytic WS_2/MoS_2 crystallites [6,7]. We will further study the adsorption of thiophene molecules on UO_2 to identify the interaction of aromatic S-containing molecules with UO_2 surfaces.

5. Conclusion

The adsorption and decomposition of H_2S molecules on polycrystalline UO_2 surface have been

studied at 100 and 300 K. Our results indicate that H_2S initially dissociates on the surface at low coverage through reaction on defect sites and O-vacancies. At 100 K, molecular H_2S can be adsorbed to a coverage of ~1 ML on the polycrystalline surface. Upon annealing, molecular H_2S desorbs at ~140 K; at ~250 K, a recombination reaction of H_2S fragments (e.g. SH) occurs, leading to further desorption of H_2S molecules. We have also found that atomic S is desorbed from the surface at ~580 K. The adsorbed S species on polycrystalline UO_2 surface are classified as molecular H_2S, SH, and atomic S; whereas molecular H_2S is mostly associated with surface U sites, dissociative S species are associated with O sites. We compare the present results with our previous study on single crystal UO_2(0 0 1), and discuss the conclusions in the context of HDS catalysis.

Acknowledgements

This work has been supported in part by the US Department of Energy (DOE), Oak Ridge Office of Site Closure (EM-32).

References

[1] T. Kabe, A. Ishihara, W. Qian, Hydrodesulfurization and Hydrodenitrogenation: Chemistry and Engineering, Kodansha: Tokyo, and Wiley-VCH: Weinheim Germany, 1999.
[2] J.M. Thomas, W.J. Thomas, Principles and practice of heterogeneous catalysis, VCH, Weinheim, 1997.
[3] A.N. Startsev, Catal. Rev. -Sci. Eng. 37 (1995) 353.
[4] T. Jirsak, J. Dvorak, J.A. Rodriguez, J. Phys. Chem. B 103 (1999) 5550.
[5] D.R. Huntley, D.R. Mullins, M.P. Wingeier, J. Phys. Chem. 100 (1996) 19620.
[6] J. Ramirez, A. Gutierrez-Alejandre, J. Catal. 170 (1997) 108.
[7] J. Ramirez, L. Cedeno, G. Busca, J. Catal. 184 (1999) 59.
[8] D. Wang, W. Qian, A. Ishihara, T. Kabe, J. Catal. 209 (2002) 266.
[9] D. Wang, X. Li, E.W. Qian, A. Ishihara, T. Kabe, Appl. Catal. A 238 (2003) 109.
[10] V.M. Kogan, N.N. Rozhdestvenskaya, I.K. Korshevets, Appl. Catal. A 234 (2002) 207.
[11] P.D. Costa, C. Potvin, J.-M. Manoli, J.-L. Lemberton, G. Petor, G. Djega-Mariadassou, J. Mol. Catal. A: Chemical 184 (2002) 323.
[12] P.T. Vasudevan, J.L.G. Fierro, Catal. Rev. -Sci. Eng. 38 (1996) 161.
[13] J. Leglise, J.N.M. van Gestel, L. Finot, J.C. Duchet, J.L. Dubois, Catal. Today 45 (1998) 347.
[14] V.E. Henrich, P.A. Cox, The Surface Science of Metal Oxides, Cambridge University Press, Cambridge, 1994.
[15] H.-J. Freund, Faraday Discuss. 114 (1999) 1.
[16] T.E. Madey, Faraday Discuss. 114 (1999) 461.
[17] X.-G. Wang, A. Chaka, M. Scheffler, Phys. Rev. Lett. 84 (2000) 3650.
[18] Y.D. Kim, J. Stultz, D.W. Goodman, J. Phys. Chem. B 106 (2002) 1515.
[19] M.A. Johnson, E.V. Stefanovich, T.N. Trung, J. Gunster, D.W. Goodman, J. Phys. Chem. B 103 (1999) 3391.
[20] H. Raza, S.P. Harte, C.A. Muryn, P.L. Wincott, G. Thornton, R. Casanova, A. Rodriguez, Surf. Sci. 366 (1996) 519.
[21] K.E. Smith, V.E. Henrich, Surf. Sci. 217 (1989) 445.
[22] J. Hrbek, J.A. Rodriguez, J. Dvorak, T. Jirsak, Coll. Czech. Chem. Comm. 66 (2001) 1149.
[23] J.A. Rodriguez, T. Jirsak, S. Chaturvedi, J. Chem. Phys. 111 (1999) 8077.
[24] J.A. Rodriguez, T. Jirsak, M. Perez, S. Chaturvedi, M. Kuhn, L. Gonzalez, A. Maiti, J. Am. Chem. Soc. 122 (2000) 12362.
[25] J.A. Rodriguez, J. Hrbek, J. Dvorak, T. Jirsak, A. Maiti, Chem. Phys. Lett. 336 (2001) 377.
[26] E.L.D. Hebenstreit, W. Hebenstreit, U. Diebold, Surf. Sci. 461 (2000) 87.
[27] E.L.D. Hebenstreit, W. Hebenstreit, U. Diebold, Surf. Sci. 470 (2001) 347.
[28] J.A. Rodriguez, J. Hrbek, Z. Chang, J. Dvorak, T. Jirsak, Phys. Rev. B 65 (2002) 235414.
[29] G.J. Hutchings, C.S. Heneghan, I.D. Hudson, S.H. Taylor, Nature 384 (1996) 341.
[30] C.S. Heneghan, G.J. Hutchings, S.R. O'Leary, S.H. Taylor, V.J. Boyd, I.D. Hudson, Catal. Today 54 (1999) 3.
[31] L.G. Gordeeva, Y.I. Aristov, E.M. Moroz, N.A. Rudana, V.I. Zaikovskii, Y.Y. Tanashev, V.N. Parmon, J. Nucl. Mater. 218 (1995) 202.
[32] H. Madhavaram, H. Idriss, J. Catal. 206 (2002) 155.
[33] S.V. Chong, H. Idriss, Surf. Sci. 504 (2002) 145.
[34] G.C. Allen, N.R. Holmes, J. Nucl. Mater. 223 (1995) 231.
[35] L.E. Cox, W.P. Ellis, Solid State Commun. 78 (1991) 1033.
[36] Q. Wu, B. Yakshinskiy, T.E. Madey, Surf. Sci. 523 (2003) 1.
[37] M.N. Hedhili, B.V. Yakshinskiy, T.E. Madey, Surf. Sci. 445 (2000) 512.
[38] G.C. Allen, P.M. Tucker, J.W. Tyler, J. Phys. Chem. 86 (1982) 224.
[39] J.A. Rodriguez, S. Chaturvedi, M. Kuhn, J. Hrbek, J. Phys. Chem. B 102 (1998) 5511.
[40] P.A. Redhead, Vacuum 12 (1962) 203.
[41] Z. Knor, Surf. Sci. 154 (1985) L233.
[42] A. Guttler, D. Kolovos-Vellianitis, T. Zecho, J. Kuppers, Surf. Sci. 516 (2002) 219.
[43] W.P. Ellis, T.N. Taylor, Surf. Sci. 91 (1980) 409.
[44] T.N. Taylor, W.P. Ellis, Surf. Sci. 107 (1981) 249.
[45] C. Muggelberg, M.R. Castell, G.A.D. Briggs, D.T. Goddard, Surf. Sci. 402–404 (1998) 673.
[46] W.P. Ellis, T.N. Taylor, Surf. Sci. 75 (1978) 279.
[47] M.R. Castell, D.S.L.C. Muggelberg, A.P. Sutton, G.A.D. Briggs, D.T. Goddard, Microsc. Microanal. 6 (2000) 324.